

Tilted Mirror for Lateral Mode Discrimination and Higher Kink-Free Power in Fiber Pump Lasers

Genlin L. Tan, *Member, IEEE*, Edward H. Sargent, and Jimmy M. Xu, *Senior Member, IEEE*

Abstract— Beam steering arising from interference between the fundamental lateral mode and higher order lateral modes limits the performance of 980-nm power lasers. In this paper, we analyze the feasibility of using a tilted mirror to discriminate against higher order modes. We calculate the reflectivity seen by different modes as a function of the thickness and tilt angle of the coating. Our results suggest that careful engineering of tilted coated mirrors represents a viable technique for improving the performance of power lasers.

Index Terms— Beam steering, discrete Fourier transform, Maxwell's equations, power laser, ridge waveguide, semiconductor lasers.

I. INTRODUCTION

BEAM STEERING due to coherent coupling and locking between the fundamental and higher order lateral modes [1], [2] is known to limit the performance of power lasers [3]–[6]. Weak waveguiding via the use of a shallow ridge is one method of suppressing these undesirable modes; however, the resulting increased sensitivity to injection effects and to inevitable variations in growth and processing is detrimental to yield and reliability.

We propose herein to take advantage of the fact that different lateral modes experience differing modal reflectivities when presented with a tilted facet mirror. In order to quantify this phenomenon and to enable thereby the design of improved devices, it is necessary to calculate accurately the reflectivities of the different lateral modes. Previous works which used mode-matching at the facet [7], [8] neglected the effect of three-dimensional mode shapes. The work of Lewin was extended to full calculation in three dimensions, but was applied only to the case of uncoated facets [9]–[13]. For the technologically important case of coated facet modal reflectivities, two-dimensional (2-D) calculations have previously been reported for the cases of normal [13]–[15] and tilted [16], [17] facets. Three-dimensional (3-D) calculations have been reported for laser amplifiers in [18] under the scalar field approximation in media with a purely real index of refraction. There exist, to our knowledge, no previous reports of full calculation of the reflectivity of 3-D modes from tilted coated facets.

To treat such a complicated three-dimensional problem, it is necessary to derive a suitably simplified model which

retains nevertheless the essential physics of the problem. The transverse optical mode distributions may be obtained either using the effective index method in two dimensions, as in [9], or 2-D finite-element method, as in FELES [21]. When considering the interaction between the mode and the tilted facet, however, account must be taken of all three components of the vector field, even in the case of the TE mode, because the tilted facet gives rise to a coupling between each of these elements [22]. We employ a generalized vector transfer matrix method [22] in order to calculate the reflected field. We take a convolution integral of the modal and reflected fields in the space–frequency domain to calculate the multimode reflectivities and their associated conversion coefficients.

In this paper, we begin by presenting the reflectivity model. We then apply our model to the calculation of the reflectivity in a standard three-layer laser structure (Section III). In Section IV, we explain the results of Section III using first-principles physical reasoning. We find that the important qualitative features of the results obtained numerically are of general applicability and technological importance. In Section V, we provide a full calculation for the case of a typical 980-nm power laser structure. In Appendix A, we give a brief proof of the principal formulas (the generalized divergence, orthogonality, and Parseval's formulas) used in the text. The derivation of an accurate recursion formula for the reflectivity of the coated facet is given in Appendix B.

II. THEORY OF MULTIPLE LATERAL MODE REFLECTIVITY

A. Reflectivity Formula for the Tilted Coated Facet

From Maxwell's equations, we can obtain the following equation which holds for both lossless media and media with loss/gain (see Appendix A):

$$\nabla \cdot (\mathbf{E}_1 \times \mathbf{H}_2 + \mathbf{H}_1 \times \mathbf{E}_2) = 0 \quad (1)$$

where $\mathbf{E}_1, \mathbf{H}_1$, and $\mathbf{E}_2, \mathbf{H}_2$ are any two different solutions of Maxwell's equations in the waveguide. We may therefore write for the reflected and incident fields,

$$\nabla \cdot (\mathbf{E}^r \times \mathbf{H}_i + \mathbf{H}^r \times \mathbf{E}_i) = 0 \quad (2)$$

Equation (2) will be our starting point in deriving a formula for the reflectivity of the coated laser facet. Fig. 1(a) shows the right terminal part of the top view of a laser waveguide along the longitudinal direction (z direction), in which S_1 is along the coated facet which is tilted with respect to the z axis. Around the facet S_1 , we introduce the artificial surfaces S_2, S_3, S_4 , which enclose a small volume of the waveguide

Manuscript received August 8, 1997; revised October 20, 1997. This work was supported in part by the Ontario Laser and Lightwave Research Centre and by Nortel Technology.

The authors are with the Department of Electrical Engineering, University of Toronto, Toronto, Ont., Canada M5S 1A4.

Publisher Item Identifier S 0018-9197(98)01093-8.

together with the facet S_1 . S_4 is the normal surface (i.e., perpendicular to the z axis) near the facet S_1 , and S_2, S_3 are auxiliary surfaces which extend far away from the waveguide. Integration of (2) over the small volume enclosed by these four surfaces and application of the divergence theorem yields

$$\int_{S_1 \dots S_4} (\mathbf{E}^r \times \mathbf{H}_i + \mathbf{H}^r \times \mathbf{E}_i) \cdot d\mathbf{s} = 0. \quad (3)$$

The guided modes under consideration decrease rapidly as they penetrate laterally out of the waveguide core. The integrals in (3) about S_2 and S_3 may therefore be neglected, leading to the equality

$$\begin{aligned} \int_{S_4} (\mathbf{E}^r \times \mathbf{H}_i + \mathbf{H}^r \times \mathbf{E}_i) \cdot d\mathbf{s} \\ = \int_{S_1} (\mathbf{E}^r \times \mathbf{H}_i + \mathbf{H}^r \times \mathbf{E}_i) \cdot d\mathbf{s}. \end{aligned} \quad (4)$$

The reflected fields at the artificial surface S_4 in the waveguide may be expanded in terms of backward normal modes

$$(\mathbf{E}^r, \mathbf{H}^r) = \sum_{\mu} R_{\mu} (\mathbf{E}_{-\mu}, \mathbf{H}_{-\mu}) \quad (5)$$

where R_{μ} is the expanding coefficient, and $\mathbf{E}_{-\mu}, \mathbf{H}_{-\mu}$ is a backward mode ($-\mu$) which is related to the forward mode (μ) according to

$$\begin{aligned} \mathbf{E}_{-\mu} &= [\mathbf{E}_{t\mu}(x, y) - \mathbf{E}_{z\mu}(x, y)] e^{-j\gamma_{\mu}z} \\ \mathbf{H}_{-\mu} &= [-\mathbf{H}_{t\mu}(x, y) + \mathbf{H}_{z\mu}(x, y)] e^{-j\gamma_{\mu}z} \end{aligned} \quad (6)$$

where $\mathbf{E}_{t\mu} = [E_{x\mu}, E_{y\mu}]$ and $\mathbf{H}_{t\mu} = [H_{x\mu}, H_{y\mu}]$ are the transverse components of the forward mode fields and $e^{j\omega t}$ time dependence has been assumed. γ_{μ} is the complex propagation constant. This yields the expanded formula

$$\begin{aligned} \int_{S_1} (\mathbf{E}_k^r \times \mathbf{H}_i + \mathbf{H}_k^r \times \mathbf{E}_i) \cdot d\mathbf{s} \\ = \sum_{j=0}^{\infty} R_{jk} \int_{S_4} (\mathbf{E}_{-j} \times \mathbf{H}_i + \mathbf{H}_{-j} \times \mathbf{E}_i) \cdot d\mathbf{s} \\ = \sum_{j=0}^{\infty} R_{jk} \int_{S_4} (\mathbf{E}_{tj} \times \mathbf{H}_{ti} - \mathbf{H}_{tj} \times \mathbf{E}_{ti}) \cdot d\mathbf{s} \end{aligned} \quad (7)$$

where R_{jk} describes the conversion of incident mode k into reflected mode j .

Since transverse modes with different indices obey the generalized orthogonality relationship at the normal surface S_4 (see Appendix A), we may write

$$\begin{aligned} \int_{-\infty}^{\infty} \int_{-\infty}^{\infty} dx dy (\mathbf{E}_{t,\nu} \times \mathbf{H}_{t,\mu} - \mathbf{H}_{t,\nu} \times \mathbf{E}_{t,\mu}) \cdot \bar{\mathbf{n}} \\ = \delta_{\nu,\mu} \quad (\nu \neq \mu). \end{aligned} \quad (8)$$

Substitution of (8) into (7) eliminates all terms on the right-hand side except those for which $i = j$:

$$\begin{aligned} \int_{S_1} (\mathbf{E}_k^r \times \mathbf{H}_i + \mathbf{H}_k^r \times \mathbf{E}_i) \cdot d\mathbf{s} \\ = R_{ik} \int_{S_4} (\mathbf{E}_{ti} \times \mathbf{H}_{ti} - \mathbf{H}_{ti} \times \mathbf{E}_{ti}) \cdot d\mathbf{s} \\ = R_{ik} \langle \mathbf{E}_{ti} \times \mathbf{H}_{ti} - \mathbf{H}_{ti} \times \mathbf{E}_{ti} \rangle \cdot \bar{\mathbf{n}} \\ = 2R_{ik} \langle \mathbf{E}_{ti} \times \mathbf{H}_{ti} \rangle \cdot \bar{\mathbf{n}} = 2N_0 R_{ik} \end{aligned} \quad (9)$$

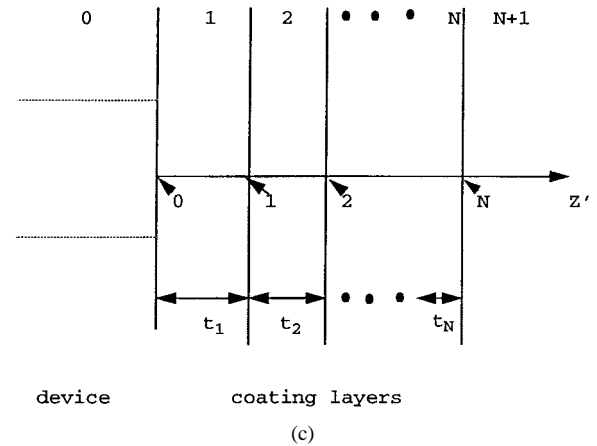
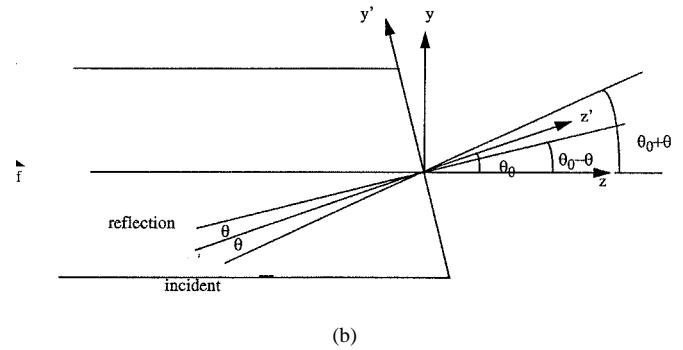
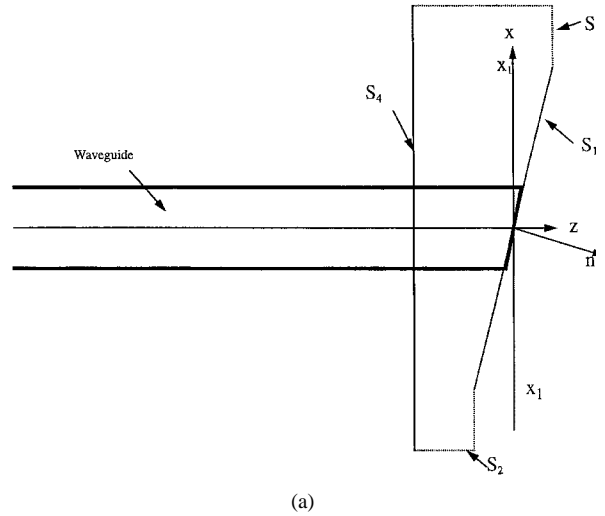


Fig. 1. (a) An integral volume enclosed by the surfaces S_1, S_2, S_3 , and S_4 . (b) The waveguide and tilted coordinate systems. (c) Equivalent system for N -layer coating to calculate the reflectivity for the plane wave. The waveguide region (the 0th layer) has been replaced with a homogeneous medium of average refractive index. The $(N+1)$ th layer is air.

where $\langle \mathbf{V} \rangle \cdot \bar{\mathbf{n}}$ denotes $\int_S \mathbf{V} \cdot \bar{\mathbf{n}} \, ds$ which $\bar{\mathbf{n}}$ is the unit normal vector of the surface S i.e.

$$N_0 = \langle (\mathbf{E}_{ti} \times \mathbf{H}_{ti}) \cdot \bar{\mathbf{n}} \rangle \quad (10)$$

Equation (9) may therefore be rewritten

$$\begin{aligned} R_{ik} &= \langle (\mathbf{E}_k^r \times \mathbf{H}_i + \mathbf{H}_k^r \times \mathbf{E}_i) \cdot \bar{\mathbf{n}}_f \rangle / 2N_0 \\ &= \langle (\mathbf{E}_k^r \times \mathbf{H}_i + \mathbf{H}_k^r \times \mathbf{E}_i)_{tg} \rangle / 2N_0 \end{aligned} \quad (11)$$

where \vec{n}_f is the unit vector normal to the coated facet and $(\mathbf{a} \times \mathbf{b})_{tg}$ denotes $\mathbf{a}_{tg} \times \mathbf{b}_{tg}$ where \mathbf{a}_{tg} (\mathbf{b}_{tg}) is the component tangential to the coated facet of vector \mathbf{a} (\mathbf{b}). If $k = i$, then (11) gives the amplitude reflection coefficient; otherwise, it gives the amplitude conversion coefficient from incident mode k to mode i . The reflectivity \mathbf{R}_{ij} is the ratio of the reflected intensity to incident intensity, $\mathbf{R}_{ii} = |\mathbf{R}_{ii}|^2$ and $\mathbf{R}_{ij} = |\mathbf{R}_{ij}|^2$. In order to calculate reflectivity and convertivity, we need therefore only consider the calculation of the amplitude reflection and conversion coefficient in the following context.

B. Calculation of the Integral of the Tangential Fields

We can convert the integral of the product of the reflected and incident field in the spatial domain to the integral of the product of their Fourier transformations in the frequency domain (see Appendix A)

$$\begin{aligned} R_{ij} &= \langle (\mathbf{E}_j^r \times \mathbf{H}_i + \mathbf{H}_j^r \times \mathbf{E}_i)_{tg} \rangle / 2N_0 \\ &= \langle (\mathbf{e}_j^r \times \mathbf{h}_i + \mathbf{h}_j^r \times \mathbf{e}_i)_{tg} \rangle / 2N_0 \end{aligned} \quad (12)$$

where \mathbf{e}, \mathbf{h} are the Fourier transforms of fields \mathbf{E}, \mathbf{H} . In the spatial frequency domain, the incident and reflected fields are proportional in magnitude but different in direction due to the tilted facet. The effective index method may be used to obtain the transverse mode, from which the field at the tilted facet may be calculated. From Fig. 1(b), we may write the field in the tilted coordinate system [23] as

$$\begin{aligned} \mathbf{E}(x, y) e^{-j\gamma z} \\ = \mathbf{E}(x, y' \cos \theta_0 - z' \sin \theta_0) e^{-j\gamma(y' \sin \theta_0 + z' \cos \theta_0)} \end{aligned} \quad (13)$$

where θ_0 is the angle between the z -axis of the waveguide and the normal direction (z') of the tilted facet. Taking the Fourier transformation for $z' = 0$ and employing the constant scaling and displacement identities yields

$$\begin{aligned} \mathbf{E}(x, y' \cos \theta_0) e^{-j\gamma y' \sin \theta_0} \\ = \frac{1}{\cos \theta_0} \int_{-\infty}^{\infty} \int_{-\infty}^{\infty} e[\xi, (\nu - \gamma \sin \theta_0 / 2\pi) / \cos \theta_0] \\ \cdot e^{-j2\pi(\xi x + \nu y)} d\xi d\nu \end{aligned} \quad (14)$$

where \mathbf{e} is the Fourier transform of the normal mode field \mathbf{E} and ξ, ν are the corresponding Fourier variables. For the reflected field, we replace γ with $-\gamma$. Defining $\nu_0 = \gamma \sin \theta_0 / 2\pi$ allows us to rewrite (12) as

$$\begin{aligned} R_{ij} &= \frac{1}{\cos^2 \theta_0} \langle \mathbf{R}(\xi, \nu) [\mathbf{e}_j(\xi, (\nu + \nu_0) / \cos \theta_0) \\ &\quad \times \mathbf{h}_i(\xi, (\nu - \nu_0) / \cos \theta_0) \\ &\quad - \mathbf{h}_j(\xi, (\nu + \nu_0) \cos \theta_0) \\ &\quad \times \mathbf{e}_i(\xi, (\nu - \nu_0) / \cos \theta_0)] \cdot \vec{n}_f \rangle / 2N_0. \end{aligned} \quad (15)$$

This convolution integral is the fundamental formula used herein. Its physical significance may be understood by first assuming θ_0 to be a small quantity so that $\cos \theta_0 \approx 1$ and $\sin \theta_0 \approx \theta_0$. If the incident field is at angle θ with respect to the normal to the tilted facet then it will be reflected at an angle $-\theta$ [see Fig 1(b)]. The incident field is at an angle $\theta + \theta_0$ to the

the z axis of the waveguide, giving it direction $\sin(\nu + \nu_0)$, while the reflected field is at angle $\theta_0 - \theta + \pi$ and has direction $\sin \gamma \sin(\pi + \theta_0 - \theta) / 2\pi = \gamma \sin(\theta - \theta_0) / 2\pi \approx \nu - \nu_0$. If we ignore for simplicity the x and ξ dimensions [see Fig. 1(b)], then we may write

$$\begin{aligned} e_t^r(\nu - \nu_0) &= R(\nu) e_{0t}(\nu + \nu_0) \\ h_t^r(\nu - \nu_0) &= -R(\nu) h_{0t}(\nu + \nu_0) \end{aligned} \quad (16)$$

where the subscript t denotes the transverse direction. The reflection coefficient of (11) may therefore be written

$$\begin{aligned} R_0 &= \langle [\mathbf{e}_t^r(\nu - \nu_0) \times \mathbf{h}_{0t}(\nu - \nu_0) \\ &\quad + \mathbf{h}_t^r(\nu - \nu_0) \times \mathbf{e}_{0t}(\nu - \nu_0)]_{tg} \rangle / (2N_0) \\ &= \langle \mathbf{R}(\nu) [\mathbf{e}_{0t}(\nu + \nu_0) \times \mathbf{h}_{0t}(\nu - \nu_0) \\ &\quad - \mathbf{h}_{0t}(\nu + \nu_0) \times \mathbf{e}_{0t}(\nu - \nu_0)]_{tg} \rangle / (2N_0). \end{aligned} \quad (17)$$

From (17) it may be seen that an incident mode with a strong angular component in the direction $\nu_1 = \gamma \sin(\theta_1) / 2\pi$ relative to the z axis will couple efficiently into a mode with a strong angular component in the direction $(\nu_1 + 2\nu_0)$. The simplifications which arise from working in the spatial frequency domain are manifested in (17) and (12), which are expressed purely in terms of incident and reflected plane waves.

C. Calculation of the Components of the Reflected Field of a Plane Wave

In order to compute the reflected field in the space-frequency domain, it is necessary only to consider the reflection of a plane wave

$$\begin{aligned} \mathbf{E}(\mathbf{x}, \mathbf{y}, z, t) &= \mathbf{E}(\mathbf{x}, \mathbf{y}) e^{j(\omega t - \gamma z)} \\ &= \mathbf{e}(\alpha, \beta) e^{j(\alpha x + \beta y)} e^{j(\omega t - \gamma z)}. \end{aligned} \quad (18)$$

The quantities $\mathbf{e}(\alpha, \beta)$ and $\mathbf{h}(\alpha, \beta)$ are related by Maxwell's equations in the time-frequency domain

$$-\omega \mu_0 h_x = \frac{\alpha \beta}{\gamma_p} e_x + \left(\gamma_p + \frac{\beta^2}{\gamma_p} \right) e_y \quad (19)$$

$$\omega \mu_0 h_y = \left(\gamma_p + \frac{\alpha^2}{\gamma_p} \right) e_x + \left(\frac{\alpha \beta}{\gamma_p} \right) e_y \quad (20)$$

where $\gamma_p = k_2 n_p^2 - \alpha^2 - \beta^2$ and n_p is the refractive index.

The facet coating is depicted in Fig. 1(c). It consists of a system of N layers, each with refractive index n_p and thickness t_p , where $(p = 1, 2, \dots, N - 1, N)$, bounded by semi-infinite media $(p = 0, p = N + 1)$. In the figure, light is incident from the left and the z' axis is normal to the facet under consideration. We may write the incident field as a superposition of plane waves which must satisfy (19) and (20). We employ the vector transfer matrix method [22] described below in order to calculate the reflected field at the facet.

Consider the vector $\mathbf{A}(z) = [e_x^F(z), e_x^B(z), e_y^F(z), e_y^B(z)]$, where the superscripts F and B denote the forward- and backward-propagating waves. Continuity across the interface $z = z_p$ may be imposed as follows:

$$\mathbf{M}_p \cdot \mathbf{A}(z_p - 0) = \mathbf{M}_{p+1} \cdot \mathbf{A}(z_p + 0), \quad p = 0, 1, \dots, N \quad (21)$$

where the transfer matrix is given by

$$\mathbf{M}_p = \begin{bmatrix} 1 & 1 & 0 & 0 \\ 0 & 0 & 1 & 1 \\ c & -c & b & -b \\ a & -a & c & -c \end{bmatrix}_p \quad (22)$$

and $a = \gamma_p + \alpha^2/\gamma_p$, $b = \gamma_p + \beta^2/\gamma_p$. Propagation across the layer (p) is represented by

$$\mathbf{A}(z_{p-1}) = \mathbf{D}_p \mathbf{A}(z_p) \quad (23)$$

where \mathbf{D}_p is a diagonal matrix and $\mathbf{D}_p = \text{diag}[\xi_p, \xi_p^{-1}, \xi_p, \xi_p^{-1}]$ with $\xi_p = \exp(j\gamma_p L_p)$. Propagation across the entire multilayer coated structure may be represented by

$$\mathbf{A}(0) = \mathbf{M} \cdot \mathbf{A}(z_N) \quad (24)$$

where

$$\mathbf{M} = \mathbf{M}_0^{-1} \cdot \mathbf{M}_1 \cdot \mathbf{D}_1 \mathbf{M}_1^{-1} \cdot \mathbf{M}_2 \cdot \mathbf{D}_2 \cdot \mathbf{M}_2^{-1} \cdots \mathbf{M}_N^{-1} \cdot \mathbf{M}_N \quad (25)$$

Matrices \mathbf{M}_p^{-1} have a simple structure

$$\mathbf{M}_p^{-1} = \frac{1}{2} \begin{bmatrix} 1 & 0 & -c/\Delta & b/\Delta \\ 1 & 0 & c/\Delta & -b/\Delta \\ 0 & 1 & a/\Delta & -c/\Delta \\ 0 & 1 & -a/\Delta & c/\Delta \end{bmatrix}_p \quad (26)$$

where $\Delta = ab - c^2 = k^2 n_p^2$.

Since there is no field incident from the right, $e_x^B(z_N) = e_y^B(z_N) = 0$. The four output variables of (24), $e_x^B(0)$, $e_y^B(0)$, $e_x^F(z_N)$, $e_y^F(z_N)$, may be written in terms of the input variables $e_x^F(0)$, $e_y^F(0)$ as follows:

$$e_x^B(0) = R_{xx} e_x^F(0) + R_{xy} e_y^F(0) \quad (27)$$

$$e_y^B(0) = R_{yx} e_x^F(0) + R_{yy} e_y^F(0) \quad (28)$$

where $R_{ij}(\alpha, \beta)$ is the amplitude reflection or coupling coefficient for the incident plane wave $e(0)$. The incident magnetic fields are related to the incident electric fields by (19) and (20), so that

$$\omega \mu_0 \begin{bmatrix} -h_x \\ h_y \end{bmatrix}_0 = \begin{bmatrix} c_0 & b_0 \\ a_0 & c_0 \end{bmatrix} \begin{bmatrix} e_x \\ e_y \end{bmatrix}_0 \quad (29)$$

The z -components of the fields are not independent variables. They may be obtained from the transverse components of the fields using Maxwell's equations

$$e_z = (\alpha e_x + \beta e_y) / \gamma_p \quad (30)$$

$$\omega \mu_0 h_z = \alpha e_y - \beta e_x \quad (31)$$

The reflected field at the facet may be written

$$\begin{bmatrix} e_x^r \\ e_y^r \end{bmatrix}_0 = \begin{bmatrix} R_{xx} & R_{xy} \\ R_{yx} & R_{yy} \end{bmatrix} \begin{bmatrix} e_x \\ e_y \end{bmatrix}_0 \quad (32)$$

and

$$\begin{bmatrix} e_z^r \end{bmatrix} = \frac{-1}{\gamma_0} (\alpha e_x^r + \beta e_y^r) = \frac{-1}{\gamma_0} [\alpha \ \beta] \begin{bmatrix} R_{xx} & R_{xy} \\ R_{yx} & R_{yy} \end{bmatrix} \begin{bmatrix} e_x \\ e_y \end{bmatrix}_0 \quad (33)$$

The magnetic field may thus be obtained from (29), (32), and (33):

$$\omega \mu_0 \begin{bmatrix} h_x^r \\ -h_y^r \end{bmatrix}_0 = \begin{bmatrix} c_0 & b_0 \\ a_0 & c_0 \end{bmatrix} \begin{bmatrix} e_x^r \\ e_y^r \end{bmatrix}_0 = \begin{bmatrix} c_0 & b_0 \\ a_0 & c_0 \end{bmatrix} \begin{bmatrix} R_{xx} & R_{xy} \\ R_{yx} & R_{yy} \end{bmatrix} \begin{bmatrix} e_x \\ e_y \end{bmatrix}_0 \quad (34)$$

$$\begin{aligned} [\omega \mu_0 h_z^r]_0 &= [\alpha e_x^r - \beta e_y^r]_0 \\ &= [-\beta \ \alpha] \begin{bmatrix} R_{xx} & R_{xy} \\ R_{yx} & R_{yy} \end{bmatrix} \begin{bmatrix} e_x \\ e_y \end{bmatrix}_0 \end{aligned} \quad (35)$$

The leftmost layer under consideration is of course nonuniform in the transverse direction because of the laser diode layer structure. In order to simplify computation an average index is obtained by weighting with the modal intensities, i.e., $\sqrt{\langle n^2 |E|^2 \rangle / \langle |E|^2 \rangle}$. In Appendix B, we provide an accurate recursion formula for determining R by considering the real 2-D nonuniform refractive index distribution. The preceding uniform index approximation is nevertheless a suitable averaging technique [22].

For the TE mode, $e_x(0) = 0$ and only $e_y(0)$ is an independent variable. For the TM mode, $e_y(0) = 0$ and only $e_x(0)$ is an independent variable. In the following discussions, we consider only the TE mode since it is by far the more relevant to laser devices.

We use the effective index method to calculate the incident field E_y as follows.

- 1) Calculate the effective indices of the center and side part along the transverse direction (TE mode) using the 1-D transfer-matrix method (TMM).
- 2) Calculate the effective index along the lateral direction (TM mode) using 1-D TMM.
- 3) Approximate the 2-D mode by the direct product of the transverse and lateral fields.

We use a standard FFT to calculate the Fourier transform of the incident field and apply (15) in order to calculate the multi-mode reflectivities in the space-frequency domain. This method has greater accuracy and requires no inverse Fourier transformation.

The present method resembles previous methods [18]–[20] in its use of overlap integrals in the spatial frequency domain. However, in addition, the present technique takes full account of 3-D components of the electromagnetic field. When applied to an example in [18], the present technique yields results with the same qualitative features as reported in [18], but with quantitative differences which increase with the tilt angle considered.

In addition, the technique described in this work allows consideration of materials with gain or loss, increasing the range of applicability of the method to quantitative consideration of active devices.

III. MULTIMODE REFLECTIVITY FOR A SIMPLE DOUBLE HETEROJUNCTION STRUCTURE

We now consider the case of a simple and generic double heterojunction laser with active layer thickness $0.2 \mu\text{m}$ and refractive index 3.45 ($\text{Al}_{0.2}\text{Ga}_{0.8}\text{As}$). The cladding of index 3.33 ($\text{Al}_{0.37}\text{Ga}_{0.63}\text{As}$) is $1.5 \mu\text{m}$ thick under the ridge and

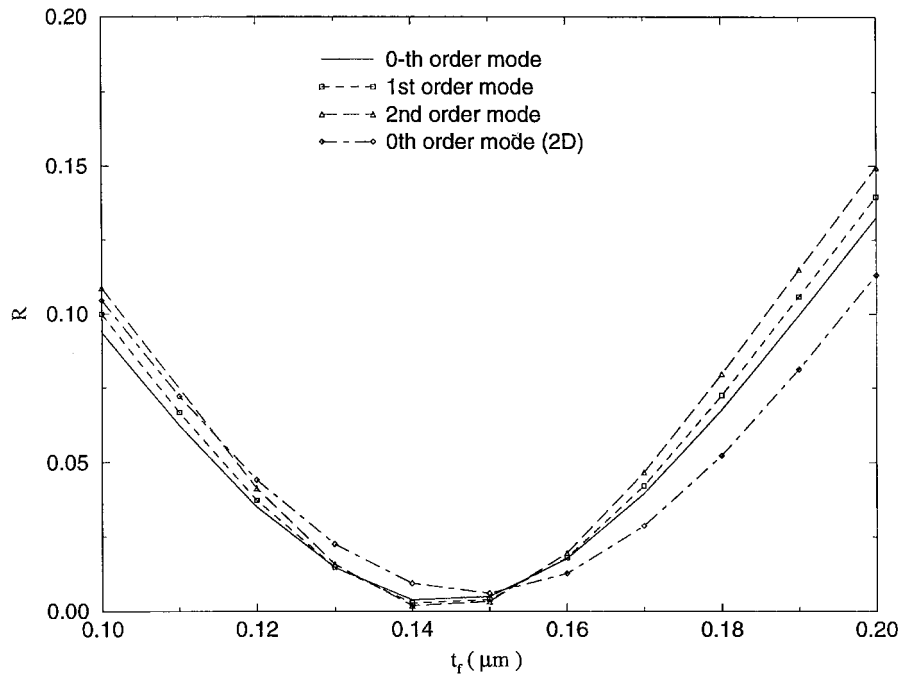


Fig. 2. Reflectivities versus coating layer thickness for a coating index n_f of 1.7 and a normal facet.

$0.2 \mu\text{m}$ to the side. The ridge width is $5 \mu\text{m}$ and our calculation extends to a total width $25.0 \mu\text{m}$.

Because of the relatively large lateral effective index difference (which could be a result of either deliberate design or injection-induced perturbations), this structure admits three lateral modes. The reflectivity of each mode is given in Fig. 2 as a function of coating thickness for a coating of refractive index $n_f = 1.7$. The reflectivity calculated using a 2-D model is also shown for comparison. We see that the 3-D reflectivity of the fundamental mode is close to that obtained from 2-D calculation, but that the curves are shifted slightly down and to the left. The 3-D reflectivity method yields a minimum in the fundamental mode reflectivity closer to $\lambda/4n_f$ than the 2-D method. Moreover, only the 3-D method permits calculation of the reflectivities of the higher order lateral modes, which are seen to exhibit greater reflectivities than the fundamental mode everywhere but in the small range for which the coating thickness t_f is close to $0.14 \mu\text{m}$ (the minimum point).

Fig. 3 gives the modal reflectivities as a function of the tilt angle of the coated facet (coating thickness $0.10 \mu\text{m}$ and index 1.7). Plotting on a logarithmic scale [Fig. 3(b)] better reveals the behavior of the reflectivities around the minimum points. The angular range within the first period is of greatest practical interest since the fundamental mode reflectivity is sufficient for lasing only in this range. At an angle of about 1.8° , the reflectivity of the first-order mode has a local minimum point and is greatly suppressed relative to that of the fundamental mode. We discuss qualitatively the physical reasons for this behavior in Section IV.

The effect of a moderate change in coating layer thickness is highlighted by comparing Fig. 3(b) ($0.10\text{-}\mu\text{m}$ -thick coating) and Fig. 3(c) ($0.14\text{-}\mu\text{m}$ -thick coating). While the absolute value of the reflectivity is altered, the angular position of the first reflectivity minimum changes only slightly. The qualita-

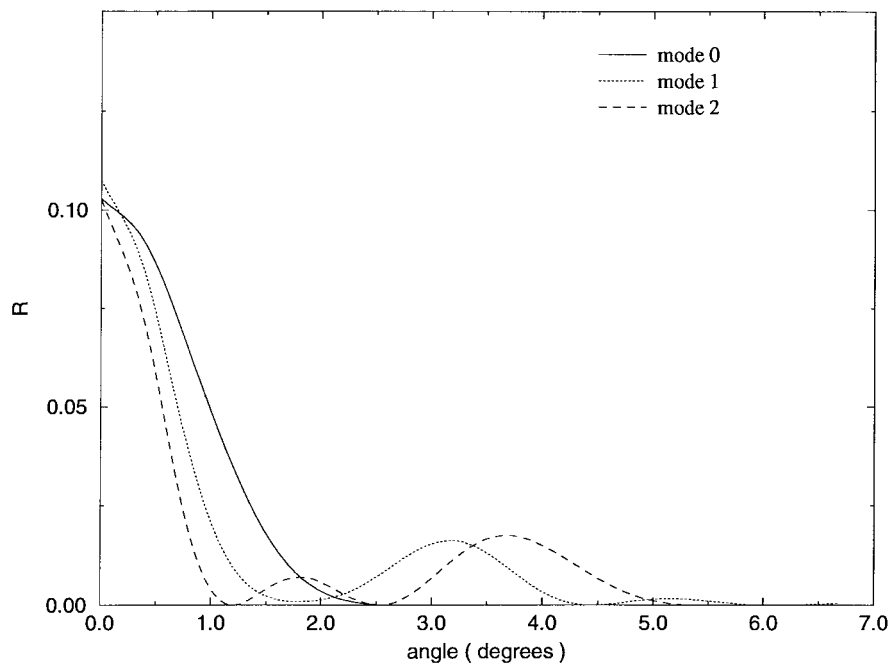
tive features of the angular dependence (wherein the first-order mode reaches a pronounced reflectivity minimum at a much smaller angle than the fundamental mode) are preserved. It is clear that the anti-reflection properties desired of the front facet of a laser may be obtained using the quarter-wave coating of Fig. 3(c) while simultaneously rejecting much more strongly the first-order mode. By enabling further explorations of the facet tilt angle and coating thickness, our model permits the design of a laser with suitably low fundamental mode threshold, high front-facet output efficiency, and strongly rejected first-order mode. The fact that the angular positions of the modal reflectivity minima are relatively insensitive to coating properties implies relaxed process tolerances and practical fabrication.

In summary, this example demonstrates that the reflectivity of the first-order mode may be strongly suppressed for tilt angles between 1° and 3° if the coating material and thickness are properly selected in accordance with the properties of the waveguide. At such small angles, the fundamental mode still experiences a sufficient reflectivity for the laser to exhibit acceptable threshold current and improved optical power output due to the use of the tilted facet.

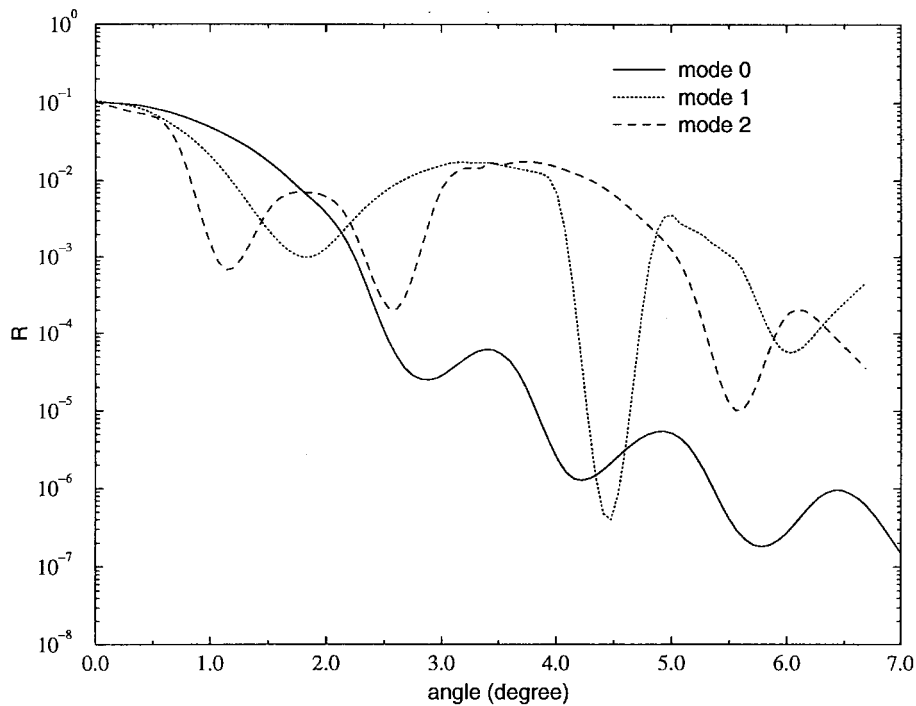
IV. QUALITATIVE DISCUSSION AND PHYSICAL GENERALIZATION

While it is necessary to employ full 3-D analysis in order to obtain quantitative solutions to the problem of modal reflectivity from a tilted, coated facet, a qualitative analysis of the results reported in Section III reveals that the heuristic features of these results are much more general than the specific case considered.

Conceptually, the modal reflectivity is related to the extent to which the components of the momentum present in the incident field are coupled back into the corresponding backward-propagating mode. In the small-angle approxima-



(a)



(b)

Fig. 3. Reflectivities of the various modes versus tilt angle of the coated facet for a coating of thickness $0.10 \mu\text{m}$ and refractive index 1.7 using (a) linear and (b) logarithmic scales.

tion, the transverse momentum and the angle of the wave vector to the waveguide axis are proportional. The effect of introducing a tilt to the facet is to shift the angular distribution of the reflected field relative to that of the incident field in direct proportion to the tilt angle.

A first step in understanding reflectivities of different modes is therefore to consider their transverse momentum distributions. In Fig. 4, we represent schematically the Fourier transforms of the lateral field distributions of the fundamental,

first-, and second-order modes. Associated with the field in the core are two symmetrical peaks (with strongly attenuated side-lobes) centered about transverse momenta k_x and $-k_x$ (where the term k_x appears in the spatial field distribution of the core, e.g., $\cos(k_x x)$ for even modes). For the fundamental lateral mode, the spacing between these peaks, $2k_x$, is comparable to or less than the width of the peaks, Δk_x . This occurs because the widths of the individual peaks are given by $2\pi/w$ (where w is the width of waveguide core), whereas for the fundamental

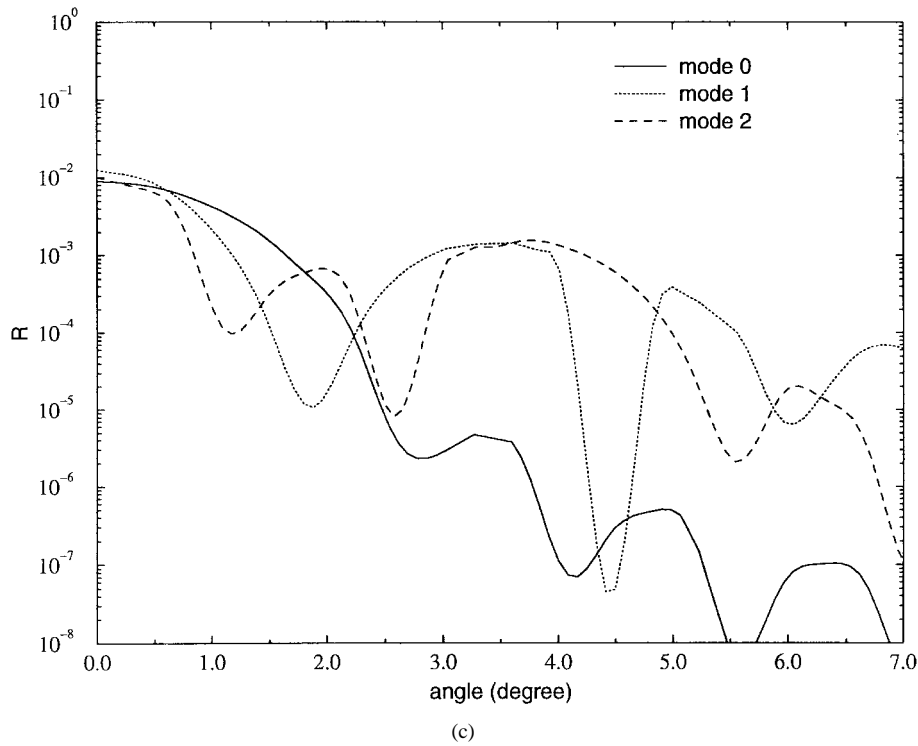


Fig. 3. (Continued.) (c) Reflectivities of the various modes versus tilt angle of the coated facet for a coating of thickness $0.10 \mu\text{m}$ and refractive index 1.7. In (c), the effect of increasing the coating to a thickness of $0.14 \mu\text{m}$ while retaining the same refractive index is shown for comparison.

mode, boundary conditions necessitate that $|k_x| \ll \pi/w$ for the case of weak guiding. As a result, the sum of the contributions from the left-going and right-going transverse momentum components is a single peak which is broader than either of the contributing peaks. In contrast, for higher order modes, the peak spacing exceeds the momentum uncertainty in the principal peaks, and distinct, narrower principal peaks appear in the total momentum distribution.

With these observations regarding the transverse momentum distribution of the various modes, we may proceed to estimate their reflectivities for different facet tilts. As argued above, tilting the facet is equivalent to imparting a shift in the transverse momentum distribution of the reflected relative to the incident field. We illustrate this process for an untilted facet in Fig. 5 in which we show the fundamental and first-order momentum distributions and associated shifts required to reach the first reflectivity minima. The shift in transverse momentum associated with the facet tilt is such that the product of the incident and reflected (shifted) momentum distributions have equal areas on either side of the vertical axis. The resulting overlap integral evaluates to zero and the first reflectivity minimum is obtained. Because the first-order mode is characterized by two distinct peaks which are narrower than the single peak of the fundamental mode, a smaller shift is required, and the first-order mode reaches a reflectivity minimum more rapidly and at a smaller angle. This accounts for the technologically important prospect of discriminating against the first-order mode while maintaining an acceptable fundamental mode reflectivity.

The remaining qualitative features of Fig. 3(b) may be understood by similar reasoning. The fact that the envelope of

the fundamental mode decreases more rapidly with increasing angle than do the higher order modes is also a consequence of the smaller average momentum of the fundamental mode. The periodic oscillations in the fundamental mode reflectivity is a result of the periodicity of the sidelobes of its momentum distribution, while the slow initial decrease in fundamental mode reflectivity with increasing angle occurs because of the greater breadth of the central lobe.

V. MODAL REFLECTIVITY FROM A TILTED COATED FACET FOR A 980-nm POWER LASER

We now turn to a discussion of modal reflectivities for a real double-quantum-well 980-nm InGaAs–GaAs–AlGaAs power laser originally designed for use with untilted facets to see how much improvement in mode selectivity may be obtained by tilting the mirrors. The structure, shown in Fig. 6, consists of $\text{In}_{0.2}\text{Ga}_{0.8}\text{As}$ wells bounded by GaAs which is in turn clad by layers of $\text{Al}_{0.2}\text{Ga}_{0.8}\text{As}$ and $\text{Al}_{0.31}\text{Ga}_{0.69}\text{As}$. The ridge width is $3 \mu\text{m}$. The design values of front and back facet reflectivities are 0.03 and 0.91.

The reflectivities seen by the fundamental and first-order modes from a coated, tilted facet are shown as a function of tilt angle for coating thicknesses for 0.10 , 0.14 , and $0.18 \mu\text{m}$ with an index of 1.7, and for $0.14 \mu\text{m}$ with an index of 1.8 in Fig. 7. The first-order mode reflectivity reaches its first minimum at approximately 1.4° irrespective of coating thickness. The angle corresponding to the first local minimum reflectivity of the first-order mode is less than in the preceding case because of the weaker lateral index guiding provided by this structure. If desired, the laser waveguiding structure could be modified to change the minimum first-order mode reflectivity angle.

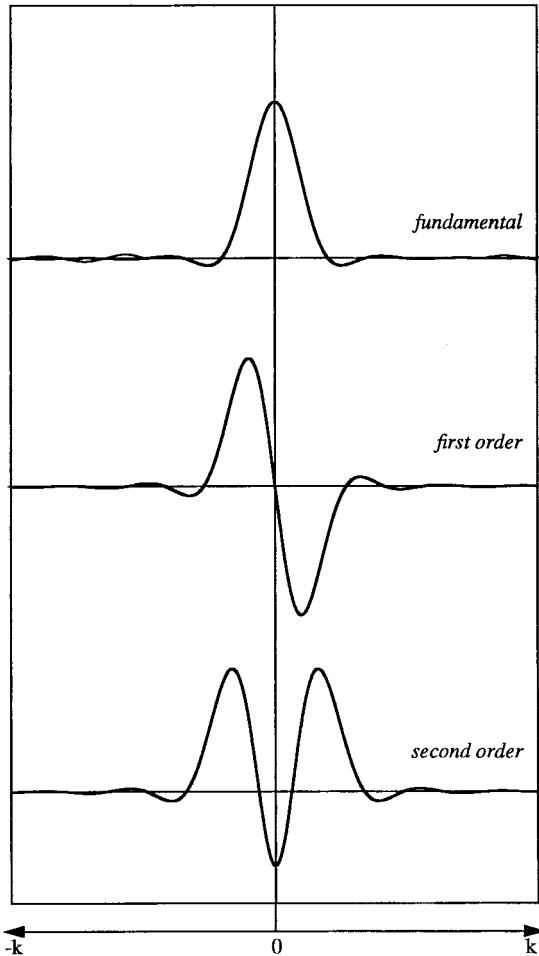


Fig. 4. Momentum-space representations of transverse modes.

The largest ratio R_0/R_1 of about 10^4 is achieved using a coating thickness of $0.16 \mu\text{m}$. This corresponds to a threefold increase in mirror loss over that of the fundamental mode. Because the fundamental mode reflectivity is equal to 0.007 in the case considered, the laser would exhibit a somewhat higher threshold; however, its far field would exhibit much greater stability than a laser with normal facets. Also, device length and even parameters can be adjusted to ensure the fundamental mode's loss thereby, threshold be at the desired value. Even when we factor in an angular uncertainty of $\pm 0.3^\circ$ due to mask alignment tolerances, the reflectivity ratio may still exceed 10^2 , corresponding to a mirror loss ratio about 2.

The reflectivity ratio R_1/R_0 at the first-order mode minimum reflectivity angle is shown in Fig. 8 as a function of coating thickness for three choices of refractive index. The strongest suppression of the first-order mode is obtained for $n_f = 1.9$ and $t_f \approx 0.143 \mu\text{m}$. The optimum tilt angle of 1.4° is a consequence of the waveguide structure; associated with a more strongly confining waveguide would be a larger tilt angle. For a buried heterostructure laser with the same lateral dimension, the optimum tilt angle would be about 3° .

Lasers with very low facet reflectivities suffer from increased sensitivity to external optical feedback. The preceding technique is equally applicable to the design of a device with tilted, coated facets whose reflectivity at normal incidence is greater than that considered in this example.

VI. CONCLUSION

By subjecting a specific laser waveguide structure to analysis using our 3-D modal reflectivity model, we have obtained a number of results which are more general than the case considered. We have seen that the first-order mode exhibits a reflectivity minimum at a smaller angle than that of the fundamental mode, and that with the selection of a suitable coating and facet tilt, the undesired first-order mode may be strongly rejected. This may be achieved at a sufficiently small tilt angle that there is an acceptably small increase in threshold and decrease in differential quantum efficiency for the fundamental mode. We have further demonstrated that the optimum tilt angle is determined much more strongly by the structure of the waveguide than by the coating thickness and refractive index. Given the excellent degree of epitaxial control of the vertical layer structure of laser waveguides, the use of a tilted facet has the potential to be a highly effective and practical way of suppressing higher order modes and achieving improved laser far-field stability and power output.

APPENDIX A

THE DERIVATION OF THE GENERALIZED DIVERGENCE, ORTHOGONALITY, AND PARSEVAL'S FORMULAS

We start with the complex Maxwell's equations for any medium:

$$\nabla \times \mathbf{E} = -j\omega\mu\mathbf{H} \quad (\text{A1})$$

$$\nabla \times \mathbf{H} = j\omega\epsilon\mathbf{E} \quad (\text{A2})$$

and consider two different solutions labeled 1 and 2. We form the dot products of \mathbf{H}_2 with (A1) with label 1, and of \mathbf{E}_1 with (A2) with the label 2, subtract the results, and obtain

$$\nabla \cdot (\mathbf{E}_1 \times \mathbf{H}_2) = -j\omega(\mathbf{E}_1 \cdot \epsilon \cdot \mathbf{E}_2 + \mathbf{H}_2 \cdot \mu \cdot \mathbf{H}_1). \quad (\text{A3})$$

Now we exchange the labels 1 and 2 in (A3) and subtract the result from (A3) to obtain

$$\begin{aligned} \nabla \cdot (\mathbf{E}_1 \times \mathbf{H}_2) - \nabla \cdot (\mathbf{E}_2 \times \mathbf{H}_1) \\ = -j\omega(\mathbf{H}_2 \cdot \mu \cdot \mathbf{H}_1 - \mathbf{H}_1 \cdot \mu \cdot \mathbf{H}_2 \\ + \mathbf{E}_1 \cdot \epsilon \cdot \mathbf{E}_2 - \mathbf{E}_2 \cdot \epsilon \cdot \mathbf{E}_1). \end{aligned} \quad (\text{A4})$$

If μ and ϵ are symmetric tensors, then the right-hand side of the above equation is zero. We have

$$\nabla \cdot (\mathbf{E}_1 \times \mathbf{H}_2 - \mathbf{E}_2 \times \mathbf{H}_1) = 0. \quad (\text{A5})$$

In general, for semiconductor material, μ is a constant and ϵ is a scalar (generally complex) in the isotropic case, or a vector in the nonisotropic case. Equation (A5) holds for both lossless media and gain/loss media, the second of which we consider in this work.

Equation (A5) is often derived (see, e.g., [21]) by starting with

$$\nabla \cdot (\mathbf{E}_1 \times \mathbf{H}_2^* - \mathbf{E}_2^* \times \mathbf{H}_1) = 0 \quad (\text{A6})$$

(where * denotes complex conjugate) which holds only for lossless media, and replacing field 2 in (A6) with its time-reversed field. This technique is not applicable to a medium with gain or loss, and the preceding derivation is therefore needed for the case of laser diode.

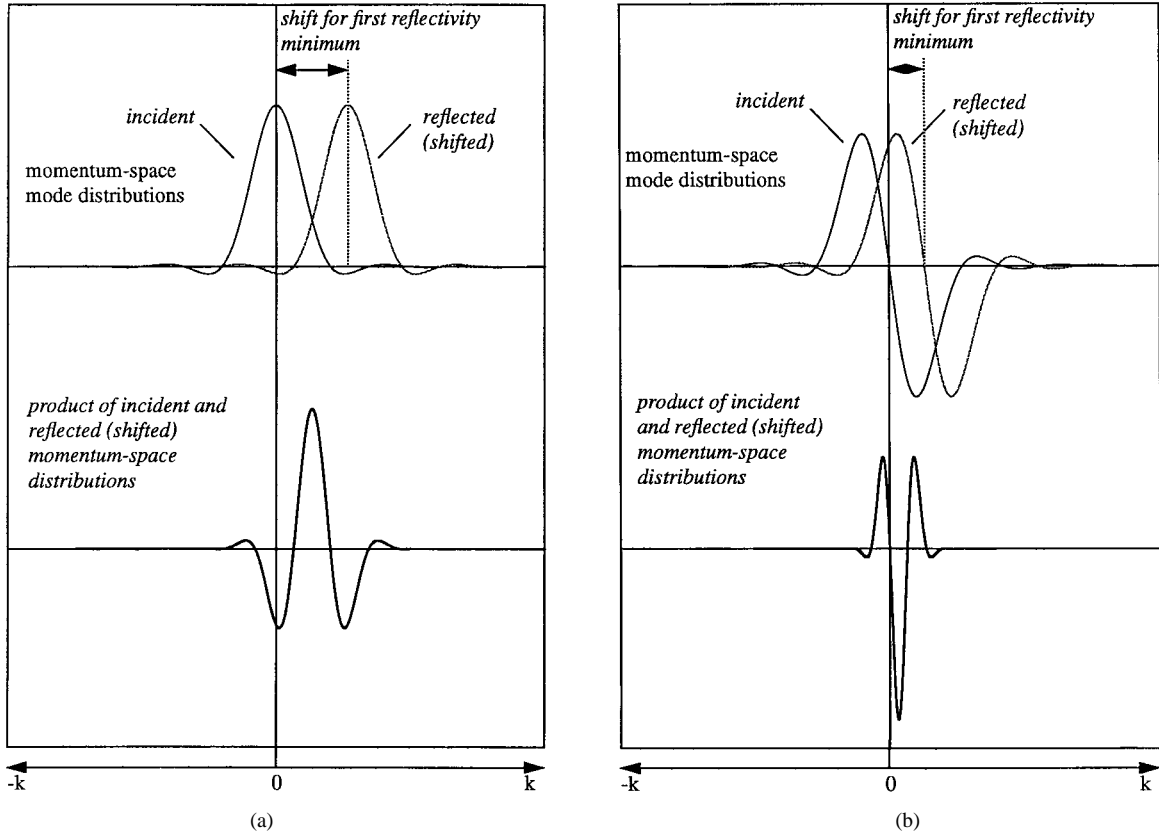


Fig. 5. Generation of the first reflectivity minima for (a) the fundamental modes and (b) the first-order modes. The shift in transverse momentum associated with the facet tilt is such that the product of the incident and reflected (shifted) momentum distributions have equal areas on either side of the vertical axis. The resulting overlap integral evaluates to zero and the first reflectivity minimum is obtained. Because the first-order mode is characterized by two distinct peaks which are narrower than the single peak of the fundamental mode, a smaller shift is required and the first-order mode reaches a reflectivity minimum more rapidly and at a smaller angle. The first-order mode may be prevented from lasing while the fundamental mode retains an acceptably low threshold.

It is well known that the modes in gain medium waveguide are not mutually orthogonal, but there does exist a generalized orthogonality relation between forward and backward normal modes considered in the text [see (8)]. To prove this, we assume that we have backward mode 1 and forward mode 2

$$\mathbf{E}_1 = \mathbf{E}_\nu(x, y) \exp(j\beta_\nu z) \quad (\text{A7a})$$

$$\mathbf{E}_2 = \mathbf{E}_\mu(x, y) \exp(-j\beta_\mu z). \quad (\text{A7b})$$

Substituting to (A5), we obtain

$$\nabla_t \cdot (\mathbf{E}_\nu \times \mathbf{H}_\mu + \mathbf{H}_\nu \times \mathbf{E}_\mu) - j(\beta_\mu - \beta_\nu)(\mathbf{E}_{t\nu} \times \mathbf{H}_{t\mu} - \mathbf{H}_{t\nu} \times \mathbf{E}_{t\mu}) = 0. \quad (\text{A8})$$

Here, we have separated the transverse (t) and the longitudinal (z) components and used the transverse del operator ∇_t . Integrating (A8) over a cross section $z = \text{const}$ of the waveguide and applying the divergence theorem to the first term, we obtain

$$\int_{-\infty}^{\infty} \int_{-\infty}^{\infty} dx dy \nabla_t \cdot \mathbf{g} = \int_c ds \mathbf{g} \cdot \mathbf{e}_t = 0 \quad (\text{A9})$$

where $\mathbf{g} = (\mathbf{E}_\nu \times \mathbf{H}_\mu + \mathbf{H}_\nu \times \mathbf{E}_\mu)_t$ and the line integral extends over an infinitely large curve enclosing the waveguide, with \mathbf{e}_t being a unit vector perpendicular to that curve. This line integral vanishes if at least one of the two modes is a guide mode with fields decaying exponentially toward infinity. The integral also vanishes when both modes are radiation modes,

as can be seen using a limiting procedure from discrete modes to continuous modes. The terms remaining after integration become (8) due to $\beta_\mu \neq \beta_\nu$.

To prove (12) (the generalized Parseval's formula that converts the integral in the spatial domain to an integral in frequency domain), we may consider 1-D scalar case without loss of generality.

$$\begin{aligned} & \int_{-\infty}^{\infty} E_j^r(x) H_i(x) dx \\ &= \int_{-\infty}^{\infty} dx \int_{-\infty}^{\infty} d\mu' e_j^r(\mu') e^{j2\pi\mu'x} \\ & \quad \cdot \int_{-\infty}^{\infty} d\mu'' h_i(\mu'') e^{-j2\pi\mu''x} \\ &= \int \int_{-\infty}^{\infty} d\mu' d\mu'' e_j^r(\mu') h_i(\mu'') \\ & \quad \cdot \int_{-\infty}^{\infty} dx e^{-j2\pi(\mu' + \mu'')x} \\ &= \int \int_{-\infty}^{\infty} d\mu' d\mu'' e_j^r(\mu') h_i(\mu'') \delta(\mu' + \mu'') \\ &= \int_{-\infty}^{\infty} e_j^r(-\mu) h_i(\mu) d\mu \\ &= \int_{-\infty}^{\infty} r(\mu) e_j(\mu) h_i(\mu) d\mu \end{aligned} \quad (\text{A10})$$

where e, h are the Fourier transform of E, H .

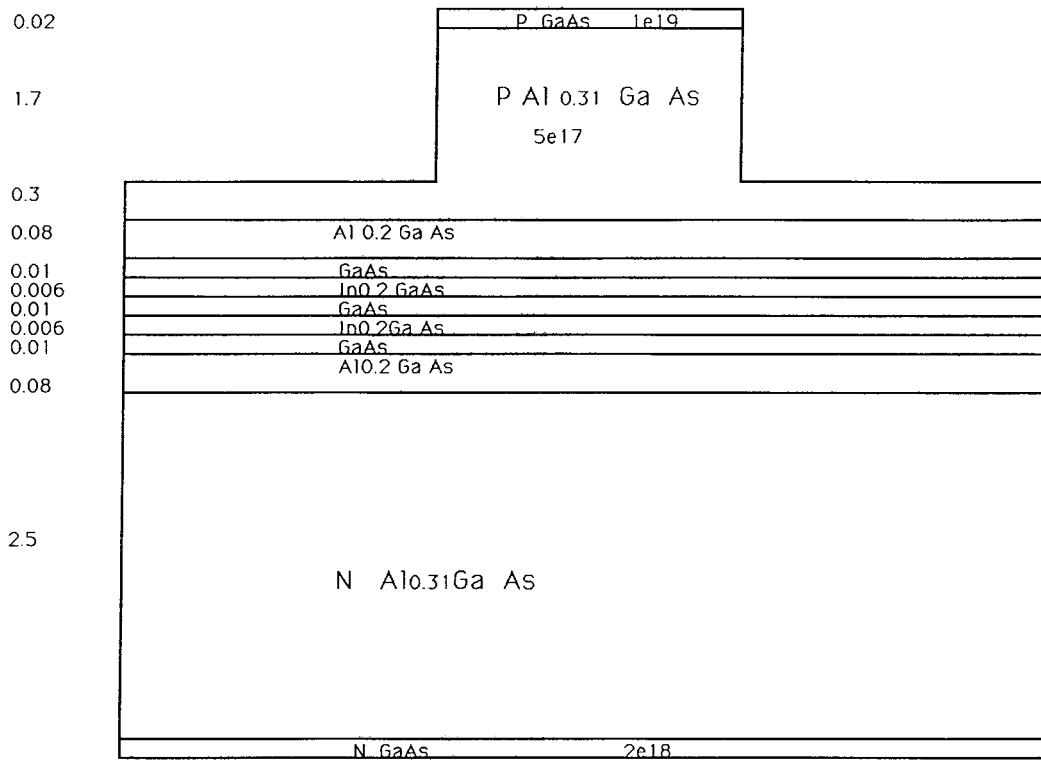


Fig. 6. 980-nm power laser structure.

APPENDIX B RECURSIVE FORMULA FOR ACCURATE CALCULATION OF MODAL REFLECTIVITY

In the calculation of the reflected field, we used an approximate equivalent constant index for the 2-D index distribution of the waveguide. We may obtain the modal reflectivity more accurately by extending the method described in [13] to the 3-D case.

The zeroth layer of Fig. 1(c), being the laser waveguide structure, has a nonuniform refractive index

$$n(x, y) = \bar{n} + \Delta n(x, y) \quad (\text{B1})$$

where \bar{n} is an equivalent or average constant index and $\Delta n(x, y)$ is the deviation from this value. In Fourier space, at interface 0, we may write

$$\sum_j \mathbf{e}_j |j\rangle + \mathbf{e}_j^r |j\rangle = \sum_j \mathbf{e}_{tj} |j\rangle \quad (\text{B2})$$

$$\sum_j \mathbf{h}_j |j\rangle + \mathbf{h}_j^r |j\rangle = \sum_j \mathbf{h}_{tj} |j\rangle \quad (\text{B3})$$

where j is the Fourier index. It follows from (29) that

$$\omega \mu_0 \begin{bmatrix} -h_x \\ h_y \end{bmatrix}_0 = \begin{bmatrix} c_0 & b_0 \\ a_0 & c_0 \end{bmatrix} \begin{bmatrix} e_x \\ e_y \end{bmatrix}_0 = P_0 \begin{bmatrix} e_x \\ e_y \end{bmatrix}_0 \quad (\text{B4})$$

We define $\mathbf{e} = [e_x, e_y]^T$ and $\mathbf{h} = [-h_x, h_y]^T$. From the expressions for $c_0, a_0,$ and $b_0,$ we may rewrite P_0 as follows:

$$P_0 = \bar{P}_0 + \Delta P_0(x, y) \quad (\text{B5})$$

where \bar{P}_0 is constant while $\Delta P_0(x, y)$ is a function of $\Delta n(x, y)$ as seen shortly. Projecting (B2) and (B3) onto

$\langle j|$ and applying (B4) and the generalized transfer matrix, we obtain

$$\begin{bmatrix} \mathbf{e} \\ \mathbf{h} \end{bmatrix}_{Z_0} = \begin{bmatrix} \mathbf{e} \\ P_0 \mathbf{e} \end{bmatrix}_{Z_0} = \begin{bmatrix} \mathbf{m}_{11} & \mathbf{m}_{12} \\ \mathbf{m}_{21} & \mathbf{m}_{22} \end{bmatrix} \begin{bmatrix} \mathbf{e} \\ P_{n+1} \mathbf{e} \end{bmatrix}_{Z_N} \quad (\text{B6})$$

where \mathbf{m}_{ij} is matrix element of the transfer matrix. The above expression may be rewritten as follows:

$$\mathbf{e}_j + \mathbf{e}_j^R = (\mathbf{m}_{11} + \mathbf{m}_{12} P_{n+1}) \mathbf{e}_{nj} = \mathbf{A} \mathbf{e}_{nj} \quad (\text{B7})$$

$$P_0 (\mathbf{e}_j - \mathbf{e}_j^R) = (\mathbf{m}_{21} + \mathbf{m}_{22} P_{n+1}) \mathbf{e}_{nj} = \mathbf{B} \mathbf{e}_{nj} \quad (\text{B8})$$

where the subscript n denotes interface n , and $\mathbf{e}_j, \mathbf{e}_j^R$ are incident and reflected fields at interface 0. It will be seen shortly that an expression for \mathbf{m}_{ij} is not required since this quantity does not enter into the final computation.

If P_0 is a constant then \mathbf{e}_j^R may be obtained by solution of (B7) and (B8):

$$\mathbf{e}_j^R = (\mathbf{A}^{-1} + \mathbf{B}^{-1} P_0)^{-1} (\mathbf{B}^{-1} P_0 - \mathbf{A}^{-1}) \mathbf{e}_j = \mathbf{R}_j \mathbf{e}_j \quad (\text{B9})$$

where \mathbf{R}_j is the amplitude reflection coefficient matrix for the plane wave incident on the coating. One way of calculating it is to use the generalized transfer matrix method (25).

If P_0 is not constant, then multiplying (B3) by $\langle j|$ and using the identity $\sum_{j'} \langle j' | j' \rangle \langle j' | = 1$, we obtain

$$\begin{aligned} \sum_{j'} \langle j | \bar{P}_0 + \Delta P_0(x, y) | j' \rangle \langle j' | (\mathbf{e}_j - \mathbf{e}_j^R) | j' \rangle \\ = \bar{P}_0 (\mathbf{e}_j - \mathbf{e}_j^R) + \sum_{j'} \langle j | \Delta P_0(x, y) | j' \rangle (\mathbf{e}_j^R - \mathbf{e}_j^R) \\ = \mathbf{B} \mathbf{e}_{nj}. \end{aligned} \quad (\text{B10})$$

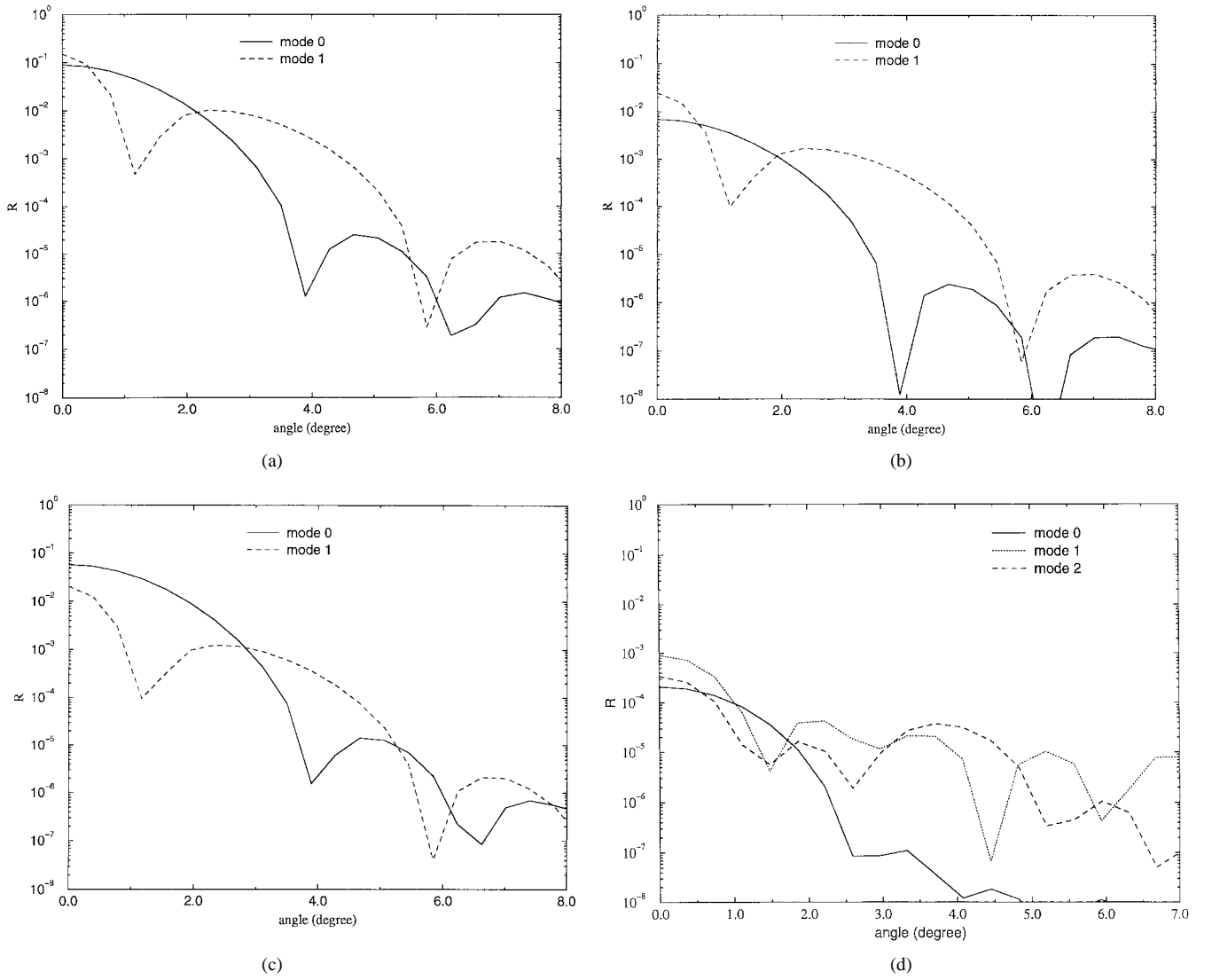


Fig. 7. Reflectivities of the fundamental and first-order modes as a function of tilt angle for a refractive index of 1.7 and coating layer thicknesses (a) 0.10, (b) 0.14, (c) 0.18 μm and an index of 1.8 for thickness (d) 0.14 μm .

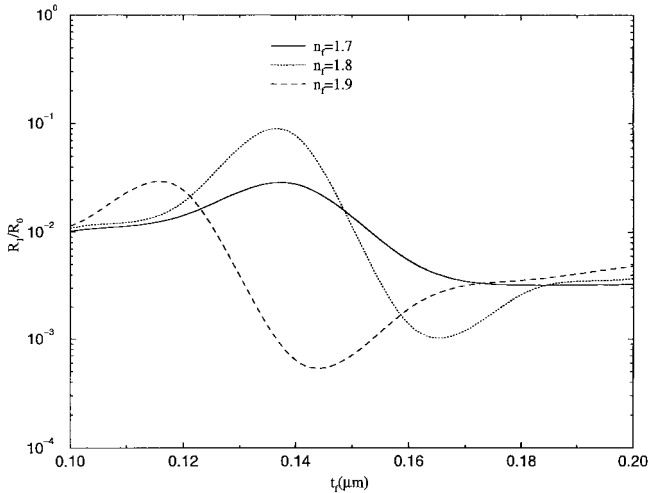


Fig. 8. Minimum modal reflectivity ratio R_1/R_0 as a function of coating layer thickness for refractive indices of 1.7, 1.8, and 1.9.

We obtain, therefore,

$$\mathbf{e}_j + \mathbf{e}_j^r = \mathbf{A}\mathbf{e}_{N_j} \quad (\text{B11})$$

$$\bar{\mathbf{P}}_0(\mathbf{e}_j - \mathbf{e}_j^r) + \sum_{j'} \Delta P_{0jj'}(\mathbf{e}_{j'} - \mathbf{e}_{j'}^r) = \mathbf{B}\mathbf{e}_{N_j}. \quad (\text{B12})$$

From (B11) and (B12), we may solve for \mathbf{e}_j^r

$$\begin{aligned} \mathbf{e}_j^r &= (\mathbf{A}^{-1} + \mathbf{B}^{-1}\bar{\mathbf{P}}_0)^{-1}(\mathbf{B}^{-1}\bar{\mathbf{P}}_0 - \mathbf{A}^{-1})\mathbf{E}_j \\ &\quad + (\mathbf{A}^{-1} + \mathbf{B}^{-1}\bar{\mathbf{P}}_0)^{-1}\mathbf{B}^{-1} \sum_{j'} \Delta P_{0jj'}(\mathbf{e}_{j'} - \mathbf{e}_{j'}^r) \\ &= \mathbf{R}_j\mathbf{e}_j + (\mathbf{R}_j + \mathbf{I})\frac{\bar{\mathbf{P}}_0^{-1}}{2} \sum_{j'} \Delta P_{0jj'}(\mathbf{e}_{j'} - \mathbf{e}_{j'}^r) \end{aligned} \quad (\text{B13})$$

where \mathbf{I} is the identity matrix and we have used the identity

$$\begin{aligned} \mathbf{R}_j + \mathbf{I} &= (\mathbf{A}^{-1} + \mathbf{B}^{-1}\bar{\mathbf{P}}_0)^{-1}(\mathbf{B}^{-1}\bar{\mathbf{P}}_0 - \mathbf{A}^{-1}) \\ &\quad + (\mathbf{A}^{-1} + \mathbf{B}^{-1}\bar{\mathbf{P}}_0)^{-1}(\mathbf{A}^{-1} + \mathbf{B}^{-1}\bar{\mathbf{P}}_0) \\ &= (\mathbf{A}^{-1} + \mathbf{B}^{-1}\bar{\mathbf{P}}_0)^{-1}\mathbf{B}^{-1}2\bar{\mathbf{P}}_0 \end{aligned} \quad (\text{B14})$$

$$\Delta P_0 = \begin{bmatrix} \alpha\beta\left(\frac{1}{r_0} - \frac{1}{\bar{r}_0}\right) & r_0 - \bar{r}_0 + \beta\beta\left(\frac{1}{r_0} - \frac{1}{\bar{r}_0}\right) \\ r_0 - \bar{r}_0 + \alpha\alpha\left(\frac{1}{r_0} - \frac{1}{\bar{r}_0}\right) & \alpha\beta\left(\frac{1}{r_0} - \frac{1}{\bar{r}_0}\right) \end{bmatrix} \quad (\text{B19})$$

where \mathbf{R}_j is the amplitude reflection matrix obtained assuming a constant refractive index in the 0th layer. From (B13), it may be seen that the reflected field only depends on \mathbf{R}_j , \bar{P}_0 and $\Delta P_{0jj'}$, and not on the matrix element m_{ij} .

We may now calculate the reflected field iteratively as follows:

1) Zeroth-order approximation:

$$\mathbf{e}_j^{r(0)} = \mathbf{R}_j \mathbf{e}_j. \quad (\text{B15})$$

2) Zeroth-order correction:

$$\Delta \mathbf{e}_j^{r(0)} = (\mathbf{R}_j + \mathbf{I})(\bar{P}_0^{-1}/2) \sum_{j'} \Delta P_{0jj'} (\mathbf{I} - \mathbf{R}) \mathbf{e}_{j'}. \quad (\text{B16})$$

3) i th-order correction obtained from the $(i-1)$ th-order correction:

$$\Delta \mathbf{e}_j^{r(i)} = \Delta \mathbf{e}_j^{r(0)} - (\mathbf{R} + \mathbf{I})(\bar{P}_0^{-1}/2) \cdot \sum_{j'} \Delta P_{0jj'} \Delta \mathbf{e}_{j'}^{r(i-1)}, \quad i = 1, 2, \dots \quad (\text{B17})$$

Consider $P_0, \bar{P}_0 = \bar{P}_0 + \Delta P_0$,

$$\bar{P}_0 = \begin{bmatrix} \frac{\alpha\beta}{\bar{r}_0} & \bar{r}_0 + \frac{\beta\beta}{\bar{r}_0} \\ \bar{r}_0 + \frac{\alpha\alpha}{\bar{r}_0} & \bar{r}_0 + \frac{\alpha\alpha}{\bar{r}_0} \end{bmatrix} \quad (\text{B18})$$

and (B19), shown at the top of the page, where

$$\begin{aligned} \bar{r}_0 &= k_0 \sqrt{\bar{n}^2 - \alpha^2 - \beta^2} \\ r_0 &= k_0 \sqrt{n(x, y)^2 - \alpha^2 - \beta^2} \\ r_0 - \bar{r}_0 &\approx \frac{k_0 \Delta n(x, y) \bar{n}}{\sqrt{\bar{n}^2 - \alpha^2 - \beta^2}} \end{aligned}$$

and

$$\frac{1}{r_0} - \frac{1}{\bar{r}_0} \approx -\frac{k_0^{-1} \Delta n(x, y) \bar{n}}{(n^2 - \alpha^2 - \beta^2)^{3/2}}$$

where α, β are the normalized space frequency variables $\xi\lambda, \nu\lambda$. The dominant term $\Delta P_{0jj'}$ in the recursive formula is

$$\begin{aligned} \Delta P_{0jj'} &= \int \Delta P_0(\xi, \nu, x, y) e^{j2\pi(\xi x + \nu y)} \\ &\quad \cdot e^{j2\pi(\xi' x + \nu' y)} dx dy \\ &= \delta P_0(\xi, \nu, \xi' - \xi, \nu' - \nu) \end{aligned} \quad (\text{B20})$$

where δP_0 is the Fourier transform of ΔP_0 . It should be noted that \bar{P}_0 and ΔP_0 are functions of the space frequency variables (ξ, ν) . It is therefore necessary to calculate J (the number of 2-D sample points) Fourier transforms of ΔP_0 , which represents an onerous computational effort. If the zeroth-order correction is not sufficiently accurate, the preceding equations make it possible to calculate $\Delta P_{0jj'}$ in a parallel manner.

ACKNOWLEDGMENT

The authors wish to thank K. Lee and R. Gordon for their assistance in the preparation of this manuscript.

REFERENCES

- [1] J. Guthrie, G. L. Tan, M. Ohkubo, T. Fukushima, Y. Ikegami, T. Ijichi, M. Irikawa, R. S. Mand, and J. M. Xu, "Beam instability in 980 nm power laser: Experiment and analysis," *IEEE Photon. Technol. Lett.*, vol. 6, pp. 1409-1411, 1994.
- [2] M. F. C. Schemmann, C. J. van der Poel, B. A. H. van Bakel, H. P. M. M. Ambrosius, and A. Valster, "Kink power in weakly index guided semiconductor lasers," *Appl. Phys. Lett.*, vol. 66, no. 8, pp. 920-922, 1995.
- [3] H. Jaeckel, G.-L. Bona, P. Buchmann, H. P. Meier, P. Vettiger, W. J. Kozlovsky, and W. Lenth, "Very high-power (425 mW) AlGaAs SQW-GRINSCH ridge laser with frequency-doubled output (41 mW at 428 nm)," *IEEE J. Quantum Electron.*, vol. 27, pp. 1560-1567, 1991.
- [4] C. H. Wu, P. S. Zory, and M. A. Emanuel, "Characterization of thin p-clad InGaAs single-quantum-well lasers," *IEEE Photon. Technol. Lett.*, vol. 7, pp. 718-720, 1995.
- [5] M. L. Xu, G. L. Tan, R. Clayton, and J. M. Xu, "Increased threshold for the first-order lateral mode lasing in low-ridge waveguide high power QW lasers," *IEEE Photon. Technol. Lett.*, vol. 8, pp. 1444-1446, 1996.
- [6] J. Guthrie, G. L. Tan, M. Ohkubo, T. Fukushima, Y. Ikegami, T. Ijichi, M. Irikawa, R. S. Mand, and J. M. Xu, "Beam steering in 980 nm high power laser diode," in *Proc. LEOS'94 Conf.*, Oct. 31-Nov. 3, 1994, vol. 2, pp. 43-44.
- [7] T. Ikegami, "Reflectivity of mode at facet and oscillation mode in double-heterostructure injection lasers," *IEEE J. Quantum Electron.*, vol. QE-8, pp. 470-476, 1972.
- [8] L. Lewin, "A method for the calculation of the radiation-pattern and mode-conversion properties of a solid-state hetero-junction laser," *IEEE Trans. Microwave Theory Tech.*, vol. MTT-23, pp. 576-585, 1975.
- [9] A. Hardy, "Formulation of two-dimensional reflectivity calculations based on the effective-index method," *J. Opt. Soc. Amer. A*, vol. 1, no. 5, pp. 550-555, 1984.
- [10] ———, "Formulation of two-dimensional reflectivity calculations for transverse-magnetic-like modes," *J. Opt. Soc. Amer. A*, vol. 1, no. 7, pp. 760-763, 1984.
- [11] ———, "Orthogonality relations of modes obtained by the effective-index method," *J. Opt. Soc. Amer. A*, vol. 1, no. 5, pp. 548-549, 1984.
- [12] D. Handelman, A. Hardy, and A. Katzir, "Reflectivity of TE modes at the facets of buried heterostructure injection lasers," *IEEE J. Quantum Electron.*, vol. QE-22, pp. 498-500, 1986.
- [13] D. R. Kaplan and P. P. Deimel, "Exact calculation of the reflection coefficient for coated waveguide devices," *AT&T Bell Lab. Tech. J.*, vol. 63, pp. 857-877, 1984.
- [14] C. Vassallo, "Reflectivity of multidielctric coatings deposited on the end facet of a weakly guiding dielectric slab waveguide," *J. Opt. Soc. Amer. A*, vol. 5, pp. 1918-1928, 1988.
- [15] ———, "Some numerical results on polarization insensitive 2-layer antireflection coatings for semiconductor optical amplifiers," *Proc. Inst. Elect. Eng.*, vol. 137, pt. J, pp. 203-204, 1990.
- [16] J. Salzman, R. J. Hawkins, and T. P. Lee, "Modal coupling in tilted-mirror waveguide lasers and amplifiers," *Opt. Lett.*, vol. 13, no. 6, pp. 455-457, 1988.
- [17] P. D. Einziger and J. Salzman, "Plane-wave spectrum approach for tilted waveguides," *Opt. Lett.*, vol. 13, no. 12, pp. 1135-1137, 1988.
- [18] B. Jaskorzynska, J. Nilsson, and L. Thylen, "Modal reflectivity of uptapered, tilted-facet, and antireflection-coated diode-laser amplifiers," *J. Opt. Soc. Amer. B*, vol. 8, pp. 484-493, 1991.
- [19] P. A. Besse, J. S. Gu, and H. Melchior, "Reflectivity minimization of semiconductor laser amplifiers with coated and angled facets considering two-dimensional beam profiles," *IEEE J. Quantum Electron.*, vol. 27, pp. 1830-1836, 1991.

- [20] J. Buus, M. C. Farries, and D. J. Robbins, "Reflectivity of coated and tilted semiconductor facets," *IEEE J. Quantum Electron.*, vol. 27, pp. 1837–1842, 1991.
- [21] G. L. Tan, N. Bewtra, K. Lee, and J. M. Xu, "A two dimensional non-isothermal finite element simulation of laser diodes," *IEEE J. Quantum Electron.*, vol. 29, pp. 822–835, 1993.
- [22] C. Vassallo, "Theory and practical calculation of antireflection coatings on semiconductor laser diode optical amplifiers," *Proc. Inst. Elect. Eng.*, vol. 137, pt. J, pp. 193–202, 1990.
- [23] H. Kogelnik, "Theory of optical waveguides," in "Guided-wave optoelectronics," spring series in *Electronics and Photonics*, Ed., T. Tamir, vol. 26, pp. 20–33, 1988.
- [24] R. Marz, *Integrated Optics: Design and Modeling*. Norwood, MA: Artech, 1995.



Genlin L. Tan (M'90) graduated from the Department of Engineering Physics, Qinghua University, China, in 1961.

Since then, he has been engaged in teaching and research in the Department of Electrical Engineering, Beijing Polytechnic University, Beijing, China, and he was a Professor. His research concerns microcomputer application, integrated circuit analysis and optimization, semiconductor device simulation, and layout optimization of IC design. He is the author or co-author of more than 40 articles and

three books and acted as a reviewer for IEEE TRANSACTIONS ON ELECTRON DEVICES, IEEE JOURNAL OF QUANTUM ELECTRONICS, and *Applied Physics*. During 1987–1988, he was a Visiting Scholar in the Department of Electrical Engineering and Computer Science of the University of California at San Diego, La Jolla. Since 1989, he has been a Senior Research Associate in the Department of Electrical Engineering, University of Toronto, Ont., Canada. His current research interests include simulation and optimization of high-speed semiconductor devices, optoelectronic devices, and integrated circuits.



Edward H. Sargent received the B.Sc.Eng. degree in engineering physics from Queen's University in 1995. He is currently working toward the Ph.D. degree in photonics in the Department of Electrical and Computer Engineering at the University of Toronto, Toronto, Ont., Canada.

Since transferring from the Master's to the doctoral program in 1996, he has authored or co-authored ten refereed journal and conference papers, taught and supervised undergraduate students, and acted as a reviewer for IEEE TRANSACTIONS ON

ELECTRON DEVICES. He spent three summers with the Advanced Technology Laboratories of Bell-Northern Research, now Nortel Technology, from 1993 to 1995. His research interests include the theory, design, and fabrication of novel optoelectronic devices.

Mr. Sargent is a member of the Optical Society of America and an ex-officio member of the Electron Devices Society Administrative Committee.



Jimmy M. Xu (M'87–SM'91) received the Ph.D. degree in electrical engineering from the University of Minnesota, Minneapolis, in 1987.

Currently, he is a Chair Professor in the Department of Electrical and Computer Engineering, University of Toronto, Toronto, Ont., Canada, with the title of the Nortel Professor of Engineering Technology. He is the Director of the Nortel Institute at the University of Toronto and is a Principal Investigator of the Ontario Laser and Lightwave Research Centre. He is also a Principal Investigator

of the Ontario Centre for Material Research and a key associate of the Information Technology Research Centre. He has authored and co-authored more than 100 refereed papers in physics and engineering journals and more than 60 refereed conference papers. He has been granted ten patents on electronics and photonic devices. His current research interests include semiconductor physics, nanostructures, quantum electronics, and compound semiconductor device design, modeling and measurements. Currently, he leads a group of 12 researchers and graduate students at the Optoelectronics Laboratory, University of Toronto, and conducts research primarily in the areas of optoelectronics, quantum electronics, nanostructure physics, heterostructure transistors, quantum-well electronics, and photonics devices, as well as large scale computer simulations. The Optoelectronic Laboratory is sponsored by Nortel and conducts research projects funded by agencies and companies in Canada, the U.S., France, and Japan. He is an Editor of the IEEE TRANSACTIONS ON ELECTRON DEVICES.

Prof. Xu was awarded the 1995 Steacie Prize for contributions to fundamental and applied quantum electronics, a 1995 Conference Board Canada-NSERC Award for "Best Practices in University-Industry R&D" (Honorable Mention), and the 1996 FCCP Award of Merit for outstanding contributions in science and technology. One of his students received the NSERC Doctoral Thesis Prize (Engineering), another was given "The Best Student Paper Award LEOS'94," and a third was awarded the Centennial Thesis Prize from the University of Toronto. He is a member of the IEEE Electron Devices Society Meeting Committee and ex-officio of the IEEE Electron Devices Society Administration Committee.